(This is a sample cover image for this issue. The actual cover is not yet available at this time.)

Spectrochimica Acta Part A: Molecular and Biomolecular Spectroscopy 95 (2012) 148–164

Contents lists available at SciVerse ScienceDirect

Spectrochimica Acta Part A: Molecular and Biomolecular Spectroscopy

journal homepage: www.elsevier.com/locate/saa

Solvent effect on the vibrational spectra of Carvedilol

Ferenc Billes [a,d,*], Hajnalka Pataki [b], Ozan Unsalan [c], Hans Mikosch [d], Balázs Vajna [b], György Marosi [b]

[a] Department of Physical Chemistry and Material Science, Budapest University of Technology and Economics, H-1521 Budapest, Budafokiút 8, Hungary
[b] Department of Organic Chemistry and Technology, Budapest University of Technology and Economics, H-1521 Budapest, Budafokiút 8, Hungary
[c] Division of Atomic and Molecular Physics, Department of Physics, Faculty of Sciences, Istanbul University, 34134 Istanbul, Turkey
[d] Institute of Chemical Technologies and Analytics, Vienna University of Technology, A-1060 Vienna, Getreidemarkt 9, Austria

ARTICLE INFO

Article history:
Received 9 January 2012
Received in revised form 23 March 2012
Accepted 5 April 2012
Available online 23 April 2012

Keywords:
Carvedilol
Molecular geometry
Vibrational spectra
Solvent effect
Quantum chemistry

ABSTRACT

Carvedilol (CRV) is an important medicament for heart arrhythmia. The aim of this work was the interpretation of its vibrational spectra with consideration on the solvent effect. Infrared and Raman spectra were recorded in solid state as well in solution. The experimental spectra were evaluated using DFT quantum chemical calculations computing the optimized structure, atomic net charges, vibrational frequencies and force constants. The same calculations were done for the molecule in DMSO and aqueous solutions applying the PCM method. The calculated force constants were scaled to the experimentally observed solid state frequencies. The characters of the vibrational modes were determined by their potential energy distributions. Solvent effects on the molecular properties were interpreted. Based on these results vibrational spectra were simulated.

Introduction

Carvedilol (CRV) is an important medicament. Being both beta- and alpha-blocker [1] it slows the heart rhythm and reduces the force of the heart's pumping, thereby lowers blood pressure and reduces heart failures. It blocks binding to the α_1-adrenergic receptors as well, resulting in further reduction of the lowers blood pressure.

CRV has enantiomers. Horiuchi et al. [2] dealt with their different effects in case of heart failures. Fujimaki et al. investigated their stereoselective presystemic metabolism [3] Takekuma et al. studied the stereoselective metabolism of the racemic form of CRV [4]. The separation of the CRV enantiomers is possible by capillary electrophoresis with laser-induced fluorescence [5].

The molecular structure of carvedilol and its physical and chemical properties are the subject of several publications.

Wen et al. [6] prepared the β-cyclodextrin inclusion complex with CRV. Molecular modeling calculations were used for prediction of its structure. The structure of the complex was experimentally determined by fluorescence spectroscopy, ^{1}H NMR and ^{13}C NMR spectroscopy.

Almeida et al. [7] calculated the full potential energy hyper surface of CRV in vacuum and in several solvents using DFT calculations at B3LYP/6-31G(d) level of theory. The solute calculations were based on the PCM theory. Lowest SCF energies, relative conformer energies, and solvent free energies were calculated. Conformers with internal hydrogen bonding did not show significant solvent effect.

The conformations of CRV in vacuum, in DMSO and in aqueous solution were studied by the same research group in a later article [8]. They found 11 torsional angles defining the conformations of CRV. They presented their optimized values for several conformations. However, they found that the number of the possible conformations is 3^{11}. (The comparison of our results did not show similarity with the 11 angles in any of Almeida's results.)

Jagannathan et al. [9] published an important article about the vibrational and electron excitation spectroscopy of CRV. They recorded infrared spectra in the 4000–400 cm^{-1} and Raman spectra in the 3500–10 cm^{-1} regions. Electron excitation spectra were recorded between 400 and 200 nm. The authors applied semi empirical methods for the calculation of the optimized geometry and the vibrational frequencies. The calculated frequencies were scaled to the experimental ones and assigned. Simulated spectra were not published.

Marques et al. [10] recorded the Raman spectra in vacuum in the 3500–275 cm^{-1} and 1750–175 cm^{-1} region. They recorded the CRV Raman spectra in DMSO solution as well, in the1750–250 cm^{-1} region at three distinct pH values. The vibrational frequencies of the molecule were calculated with HF method and 3-21G level of

* Corresponding author at: Department of Physical Chemistry and Material Science, Budapest University of Technology and Economics, H-1521 Budapest, Budafokiút 8, Hungary.
E-mail addresses: fbilles@mail.bme.hu (F. Billes), patakihajni@gmail.com (H. Pataki), unsalan@istanbul.edu.tr (O. Unsalan), hans.mikosch@tuwien.ac.at (H. Mikosch), balazs.vajna@gmail.com (B. Vajna), gmarosi@mail.bme.hu (G. Marosi).

1386-1425/$ - see front matter © 2012 Elsevier B.V. All rights reserved.
http://dx.doi.org/10.1016/j.saa.2012.04.029

theory. A very simple scaling method was used. All calculated frequencies over 400 cm^{-1} were multiplied by a constant factor. Neither normal coordinate analysis and PED calculations, nor simulated spectra were published in the mentioned paper.

Chen et al. [11] also determined the X-ray structure of CRV with single crystal diffraction method.

Yathirajan et al. presented data about the X-ray structure of CRV polymorphs [12]. According to both measurements the CRV crystal is monoclinic (belonging to the space group $P2_1c$). However, the measured torsional angles along the chain (see Fig. 1) and the cell parameters are different. This means that the chain is flexible during the preparation of the crystal. Regarding the conformations of CRV see also Ref. [8].

Materials and methods

CRV was purchased from Symed Labs (Hyderabad, India). DMSO ($\geqslant$99% purity) was obtained from Merck (Darmstadt, Germany). Solutions were prepared by dissolving CRV in DMSO and separately in triple distilled water until saturation.

Transmission infrared spectra were recorded from the solid samples using a Bruker Tensor 37 type spectrometer (Bruker Optik GmbH, Ettlingen, Germany) equipped with a deuterated triglycine sulfate detector with 256 scans per spectrum. The spectral range was 400–4000 cm^{-1} with 4 cm^{-1} resolution.

Raman and Attenuated Total Reflection infrared spectra from all solid samples and solutions were obtained with a Horiba Jobin Yvon Labram-IR microscope (Horiba Jobin Yvon, Lyon, France) equipped with an IlluminatIR module (Smiths Detection, Danbury, USA) and an Olympus BX-40 microscope (Olympus Corporation, Tokyo, Japan). ATR infrared spectra were collected with 256 scans using an ATR diamond objective and MCT detector, at the spectral range of 650–4000 cm^{-1} with 4 cm^{-1} resolution. Raman spectra were collected using an external 532 nm frequency-doubled Nd-YAG laser source. An objective of 10× magnification was used for optical scanning and spectrum acquisition. The description of the instrument is given elsewhere [13]. All spectra were obtained in the spectral range of 500–3700 cm^{-1} with approximately 3 cm^{-1} resolution provided by a grating monochromator of 1800 groove/mm at multiple spectrograph positions. Acquisition time for solid samples was 5 s and four spectra were accumulated at each measured point. Solutions were measured in a cuvette with the same acquisition time and 15 accumulations.

Carvedilol is practically insoluble in water. Therefore we could not record neither the infrared, nor the Raman spectra of the aqueous solution.

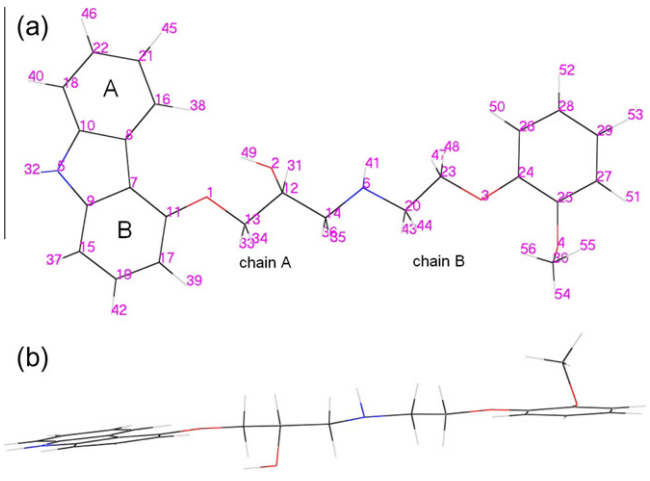

Fig. 1. CRV molecule: (a) plane view and numbering of the atoms and (b) side view.

Calculations

Quantum chemical calculations were carried out using the Gaussian 03 program package [14] with the Density Functional Theory applying the Becke3LYP functional and the 6-31G(d,p) basis set [15,16]. Optimized geometry, Mulliken's [17] and NBO/NPA [18,19] atomic net charges were computed. The second derivative of the molecular energy to the Cartesian coordinates gave the vibrational force constants and, applying the calculated optimized molecular geometry and the atomic weights, the vibrational frequencies as well.

Similar calculations were applied for the aqueous and DMSO solutions of CRV. Tomasi's polarizable continuum model (PCM) was used [20] for these computations.

The calculated vibrational frequencies were fitted to the experimental ones. For this purpose the calculated vibrational force constants were transformed into the system of defined internal (symmetry) coordinates (see about the definition of the internal (symmetry) coordinates *Vibrational force constants*). These force constants were scaled to the experimental frequencies of the normal modes.

A home-made method was applied for scaling [21]. The input data of the program are the force constant (F) and the inverse kinetic energy (G) matrices, the vector of the measured vibrational frequencies and the starting values of the scale factors. It is supposed that the chemically similar internal (symmetric) coordinates (i.e. the ones belonging to the same chemical group) have the same scale factor. For this reason the 162 internal (symmetric) coordinates of CRV were divided into groups according to the composition of the corresponding chemical group (e.g. CH, OH, NH, etc.) and type of motion (stretching, in-plane bending, o.o.p. bending, torsion). In this way 22 groups were found. The program calculates the scaled F matrix and using the G matrix as well, the eigenvalues of GF and the mean values of the measured and calculated frequencies. The scale factor was varied until the minimal deviation was found. This process was repeated for all internal coordinate groups (in our case 22). The thus yielded scale factor set was used as input for the calculations with the next coordinate set. The final outcome was the scale factor set showing the minimal deviation between the simulated and the experimental spectra. It is possible that more than one functional group have the same scale factor, which explains the fact that only 16 scale factor data were numerically different in our case. The calculated force constants were scaled to the measured vibrational frequencies of the solid CRV. The same scale factors were transferred for the solutes, since we could not measure a full frequency set of the DMSO solution, and the measurement of the aqueous solution was unavailable due to the very low solubility of CRV in water.

For the characterization of the potential energy distributions (PED) of the vibrational modes, further calculations were carried out with a homemade program. Based on the scaled frequencies and the calculated integrated intensities, simulated spectra were calculated using a homemade program, supposing Lorentz band shapes and 15 cm^{-1} FWHH. The calculated Raman activities are comparable to the experimental Raman intensities if they are corrected with the consideration of the excitation wavelength used in the experiment. Therefore the calculated Raman activities (S_i) were transferred to the excitation wavenumber (ν_0) of the experimental spectra [22]:

$$I_i = f\frac{(\nu_0-\nu_i)^4}{\nu_i\left[1-\exp\left(-\frac{hc\nu_i}{kT}\right)\right]}S_i \quad (1)$$

ν_1 is the wavenumber of the actual normal mode and f is an arbitrary factor. The Raman spectra presented in Tables 2–4 are corrected using this equation.

Results and discussion

Molecular structure

The CRV molecule contains a long chain and two aromatic systems on its two ends (Fig. 1). The optimized geometric data are given in Table 1 and in the Supplementary Table 1S.

The X-ray structure of the molecule was measured with single crystal diffraction by Chen et al. [11]. They found that the crystal is composed of a pair of enantiomers with hydrogen bonds between them. The crystal is mono-clinic within the space group $P2_1/c$.

The calculated geometric parameters of the molecules were presented by Jagannathan et al. [9]. For these calculations they used two semi empirical quantum chemical methods, AM1 and PM3 and compared their results to the experimental ones [11]. However, they published only the bond lengths and valence angles of the molecular skeleton.

As already mentioned, we calculated the molecular geometry of the molecule in vacuum (isolated molecule), and as solute in water and in DMSO. Table 1 contains selected optimized bond lengths and valence angles coupled to skeleton and movable hydrogen atoms. A full list of the calculated optimized parameters is found in the Supplementary Table 1S.

Comparing our results according Table 1, there are only small deviations in the geometric parameters of the isolated molecule and those of the CRV solutes in aqueous (according to Ref. [18] $\varepsilon = 78.39$) and DMSO ($\varepsilon = 46.7$, see Ref. [18]) solutions. The largest deviations are in the magnitude of 0.01 Å or 1–2°. The changes in the bond lengths for the O2–C12, O2–H49, N5–H32 and N6–H41 are worth mentioning. The deviations increase in the following direction: isolated molecule → DMSO solute → aqueous solute. Larger deviations are observable for the O1–C13–C12 and the C14–N6–C20 angles. The calculated semi empirical data sometimes differ from ours, e.g. this for the PM3 N5–C9 bond length is about 0.05 Å. The experimental geometric parameters are close to our calculated ones but a thorough investigation has not been carried out earlier regarding the different molecular environments.

Some dihedral angles around the heteroatoms show also large deviations from our vacuum structure under the solvent effects, more than 10°, see the changes in the C7–O1–C11–C13 angle (Supplementary Table 1S).

It should be noted that the addition of some solvent molecule to the studied one may improve the solvent effect. However, this would increase the number of atoms and therefore the necessary calculation time. If the studied molecule is small, such as glycidol (8 atoms) [23] or methyl lactate (16 atoms) [24], the addition of 1–2 water molecules leads to higher computation time but it remains acceptable. However, since Carvedilol has 56 atoms and at least six water or DMSO molecules would have to be added, the necessary computation time would be multiplied. Besides, the definition of so many necessary internal coordinates (216 and 316 coordinates) would also exceed current computational limitations. Furthermore, the corresponding bonds would overlap in the solvent spectrum. For all these reasons the solvent effect was only considered using the PCM method (we dealt with the problem of the common application of the PCM method with added solute molecules for methanol in our former publication [25]).

Atomic net charges

Both Mulliken's net atomic charges [17] and the natural NBO/NPA atomic charges [18,19] were calculated. The results are listed in Table 2.

The comparison between Mulliken's net charges and the atomic natural ones is not an easy task since these two methods have quite different theoretical backgrounds. The results show remarkable differences between the Mulliken's and the NBO charges.

The definition of Mulliken's charges is based on population analysis. The *Mulliken population analysis* provides a partitioning of either the total charge density or an orbital density. The number of the electrons in the molecule (N) is the integral of the charge density over the space. N is partitioned for all atoms, the overlap population is also considered. According to the theory, the overlap population of atoms A and B is divided between the two atoms in half-to-half ratio. This is one weak point of the theory. The other weak point is its strong dependence on the applied basis set. Our Mulliken's atomic net charges are comparable since the same basis set was used for both the isolated and the solute compounds. The atomic net charge is the difference between the calculated number of electrons belonging to the atom in the molecule and the number of electrons of the isolated atom.

The natural atomic charge is based on the theory of *natural population analysis*. The analysis is carried out with natural bond orbitals (NBO). They are linear combinations of the natural atomic orbitals. The derivation of a valence-shell atomic orbital (NAO) involves diagonalization of the localized block of the full density matrix of a given molecule associated with basis functions on the atom. A distinguishing feature of NAOs is that they meet the simultaneous requirement of orthonormality and maximum occupancy. In a polyatomic molecule NAOs mostly retain one-center character, and thus they are optimal for describing the molecular electron density around each atomic center. Natural bond orbitals are linear combinations of NAOs of two bonded atoms. The natural population analysis satisfies Pauli's exclusion principle and solves the basis set dependence problem of the Mulliken's population analysis.

Both Mullliken's and NBO atomic net charges of CRV and its solutes are listed in Table 2. Looking at the table at first glance the values and solvent effect of the heteroatom charges seem interesting. Although the numerical values of the net charges are different, the tendency of the solvent effect is similar. A large effect is observable on atom O2, where the charge becomes more negative with increasing dielectric constant, the shifts are about 0.04 atomic charge unit (a.ch.u) from vacuum to aqueous solvent. The shift is according the NBO/NPA calculations −0.036 a.ch.u. from vacuum to DMSO solute, and only −0.004 a.ch.u from DMSO to water solvent. The corresponding Mulliken's net charges show similar effect both in magnitude and in tendency. Both O2 and O4 are neither in the long chain, nor in the rings. The effects on atom O4 are similar, but the charge shifts are a little smaller. However, atoms O1 and O3 show only small solvent effects. The difference between the NBO and Mulliken's charges is for O2 surprising large (it is an OH oxygen), about −0.2 a.ch.u., while for all other oxygen atoms this difference is only about 0.01–0.02 a.ch.u. (absolute values).

Large solvent effect shows N6 (aliphatic NH), −0.029 a.ch.u. in case of NBO calculations, −0.047 a.ch.u. is the Mulliken's effect. The two solvent-to-solvent effects are zero for both calculations. The other nitrogen atom, N5 (aromatic NH) shows smaller solvent effects. It is, however interesting, comparing the Mulliken's and NBO charges of the nitrogen atoms, the absolute NBO net charge values for N5 are significantly higher than the Mullikens'. However, this is opposite case for atom N6.

Atomic net charges of almost all hydrogen atoms show strong solvent effect. Above all, the changes for movable hydrogens in O2–H41 and N5–H32 bonds are remarkable. The large effect is also here between the isolated and the solute charges, while the solute-to-solute effect is negligible or smaller than 0.0005 a.ch.u. Some other hydrogen atom charges show similar notable solvent effect: H31, H40, H42, H45, H46, H47, H48, H49, H50, H51, H52, H53 and H55 (C–H bond hydrogen atoms). These changes reflect the very

Table 1
Selected optimized geometric parameters of the carvedilol molecule.

Parameter[a]	Parameter values[b,c]					
	Calculated					Measured[f]
	Isolated molecule			As solute		
	DFT[d]	AM1[e]	PM3[e]	DMSO solution[d]	Aqueous solution[d]	
r (1,11)	1.369	1.381	1.389	1.369	1.369	1.372
r (1,13)	1.428	1.433	1.429	1.433	1.434	1.431
r (2,12)	1.416	1.417	1.413	1.424	1.423	1.430
r (2,49)	0.968	0.967	0.948	0.974	0.977	
r (3,23)	1.424	1.440	1.421	1.430	1.430	1.424
r (3,24)	1.367	1.387	1.391	1.365	1.365	1.368
r (4,25)	1.376	1.387	1.393	1.380	1.381	1.365
r (4,30)	1.429	1.429	1.411	1.434	1.435	1.429
r (5,9)	1.385	1.407	1.435	1.382	1.382	1.374
r (5,10)	1.387	1.410	1.435	1.384	1.383	1.382
r (5,32)	1.007	0.987	0.991	1.021	1.022	
r (6,41)	1.018	1.004	0.999	1.027	1.027	
r (6,14)	1.457	1.441	1.477	1.463	1.462	1.459
r (6,20)	1.457	1.451	1.484	1.461	1.460	1.462
r (7,8)	1.448			1.449	1.449	
r (7,9)	1.417			1.420	1.420	
r (7,11)	1.406	1.399	1.398	1.409	1.409	1.394
r (8,10)	1.422	1.450	1.453	1.424	1.425	1.437
r (8,16)	1.401	1.388	1.390	1.403	1.403	1.398
r (9,15)	1.399	1.400	1.393	1.401	1.401	1.391
r (10,18)	1.396	1.397	1.392	1.398	1.399	1.384
r (11,17)	1.395	1.401	1.399	1.397	1.397	1.383
r (12,13)	1.528	1.533	1.546	1.525	1.525	1.514
r (12,14)	1.527	1.543	1.544	1.527	1.528	1.518
r (15,19)	1.389	1.391	1.390	1.390	1.390	1.363
r (16,21)	1.392	1.395	1.390	1.393	1.394	1.374
r (17,19)	1.407	1.398	1.396	1.409	1.409	1.395
r (18,22)	1.393	1.394	1.390	1.394	1.394	1.362
r (20,23)	1.524	1.534	1.533	1.523	1.523	1.497
r (21,22)	1.405	1.399	1.398	1.408	1.408	1.385
r (24,25)	1.414	1.408	1.408	1.414	1.414	1.394
r (24,26)	1.398	1.402	1.400	1.399	1.399	1.371
r (25,27)	1.391	1.402	1.399	1.392	1.392	1.370
r (26,28)	1.399	1.393	1.390	1.400	1.400	1.408
r (26,50)	1.084			1.085	1.086	
r (27,29)	1.398	1.392	1.390	1.399	1.399	1.357
r (28,29)	1.391	1.396	1.392	1.393	1.393	1.360
φ (11,1,13)	119.3	116.0	112.6	118.7	118.6	118.9
φ (23,3,24)	118.5	114.4	118.4	118.6	118.6	113.1
φ (25,4,30)	115.6	113.9	113.3	115.0	114.9	117.9
φ (9,5,10)	109.8	107.6	106.1	109.6	109.6	109.1
φ (14,6,20)	113.7	115.0	111.7	111.9	112.3	114.3
φ (9,7,11)	118.9	119.0	118.7	119.0	119.0	119.5
φ (7,8,10)	106.3	106.4	107.2	106.2	106.2	106.8
φ (5,9,7)	108.1	109.5	109.4	108.5	108.5	108.5
φ (5,10,8)	108.4	109.5	109.5	108.7	108.7	108.0
φ (2,12,13)	110.1	104.9	106.4	110.8	111.0	106.8
φ (1,13,12)	105.8	109.0	110.4	106.7	107.0	109.1
φ (6,14,12)	111.6	115.7	112.4	111.9	111.8	116.8
φ (9,15,19)	117.0	117.8	117.7	117.0	116.9	117.4
φ (8,16,21)	119.1	118.8	118.3	119.1	119.1	119.0
φ (11,17,19)	120.1	120.3	120.4	120.1	120.2	119.6
φ (10,18,22)	117.6	117.8	117.5	117.7	117.7	117.7
φ (15,19,17)	122.2	122.2	121.6	122.3	122.3	122.7
φ (6,20,23)	109.6	109.3	111.4	110.1	109.8	111.9
φ (16,21,22)	120.9	121.1	121.3	120.9	120.9	120.9
φ (18,22,21)	121.3	121.7	121.4	121.3	121.3	121.8
φ (3,23,20)	107.4	111.9	106.3	107.0	107.2	104.7
φ (25,24,26)	119.3	119.9	120.0	119.2	119.2	119.9
φ (24,25,27)	119.7	119.7	119.9	120.0	120.0	119.7
φ (24,26,28)	120.2	119.9	119.8	120.1	120.1	125.1
φ (25,27,29)	120.9	120.4	121.3	120.7	120.6	120.4
φ (27,29,28)	119.4	120.4	120.5	119.4	119.4	119.9

[a] *r*: bond length; γ: valence angle.
[b] For the atom numbering see Fig. 1.
[c] Distances in angstroms; angles in degrees.
[d] This work, Becke3LYP/6-31G(d,p).
[e] Ref. [8].
[f] Ref. [10].

Table 2
Atomic net charges in the carvedilol molecule (atomic units).

Sl. No.	Atom type	Mulliken's[a]			NBO[b]		
		Isolated	In DMSO	In water	Isolated	In DMSO	In water
1	O	−0.568	−0.565	−0.565	−0.548	−0.549	−0.548
2	O	−0.540	−0.586	−0.589	−0.755	−0.790	−0.794
3	O	−0.540	−0.547	−0.548	−0.535	−0.540	−0.540
4	O	−0.529	−0.553	−0.554	−0.551	−0.570	−0.571
5	N	−0.724	−0.715	−0.714	−0.569	−0.576	−0.576
6	N	−0.516	−0.563	−0.563	−0.688	−0.717	−0.717
7	C	0.007	−0.006	−0.007	−0.124	−0.140	−0.141
8	C	0.068	0.047	0.045	−0.083	−0.097	−0.097
9	C	0.305	0.284	0.283	0.190	0.182	0.182
10	C	0.303	0.283	0.282	0.176	0.169	0.169
11	C	0.305	0.292	0.292	0.355	0.346	0.346
12	C	0.129	0.121	0.119	0.076	0.069	0.069
13	C	0.057	0.040	0.043	−0.137	−0.143	−0.142
14	C	−0.009	−0.018	−0.019	−0.279	−0.285	−0.284
15	C	−0.115	−0.146	−0.146	−0.299	−0.309	−0.310
16	C	−0.132	−0.156	−0.160	−0.210	−0.224	−0.225
17	C	−0.147	−0.175	−0.177	−0.349	−0.360	−0.362
18	C	−0.115	−0.144	−0.144	−0.277	−0.285	−0.285
19	C	−0.105	−0.134	−0.135	−0.212	−0.226	−0.226
20	C	−0.053	−0.053	−0.053	−0.276	−0.281	−0.281
21	C	−0.104	−0.134	−0.135	−0.263	−0.281	−0.282
22	C	−0.096	−0.126	−0.126	−0.231	−0.248	−0.248
23	C	0.058	0.040	0.041	−0.112	−0.118	−0.119
24	C	0.341	0.336	0.336	0.284	0.281	0.281
25	C	0.283	0.270	0.268	0.268	0.255	0.254
26	C	−0.140	−0.162	−0.163	−0.317	−0.324	−0.324
27	C	−0.109	−0.132	−0.133	−0.263	−0.275	−0.275
28	C	−0.096	−0.122	−0.123	−0.235	−0.244	−0.244
29	C	−0.098	−0.128	−0.128	−0.258	−0.271	−0.271
30	C	−0.075	−0.087	−0.088	−0.316	−0.321	−0.321
31	H	0.080	0.108	0.109	0.208	0.226	0.227
32	H	0.255	0.320	0.321	0.436	0.482	0.483
33	H	0.112	0.123	0.123	0.220	0.225	0.225
34	H	0.101	0.121	0.119	0.219	0.231	0.230
35	H	0.067	0.089	0.089	0.199	0.213	0.213
36	H	0.117	0.114	0.113	0.239	0.235	0.235
37	H	0.078	0.115	0.116	0.240	0.259	0.260
38	H	0.088	0.101	0.105	0.243	0.251	0.253
39	H	0.084	0.114	0.116	0.242	0.256	0.257
40	H	0.079	0.118	0.118	0.238	0.258	0.259
41	H	0.233	0.278	0.278	0.378	0.409	0.409
42	H	0.085	0.113	0.114	0.242	0.256	0.256
43	H	0.122	0.120	0.119	0.238	0.236	0.236
44	H	0.085	0.095	0.095	0.204	0.209	0.210
45	H	0.080	0.103	0.104	0.240	0.251	0.251
46	H	0.082	0.108	0.109	0.240	0.253	0.253
47	H	0.122	0.121	0.121	0.225	0.224	0.223
48	H	0.092	0.118	0.119	0.204	0.219	0.219
49	H	0.320	0.341	0.347	0.488	0.507	0.512
50	H	0.092	0.124	0.126	0.243	0.258	0.260
51	H	0.090	0.114	0.115	0.249	0.261	0.261
52	H	0.083	0.115	0.115	0.240	0.255	0.256
53	H	0.081	0.112	0.113	0.240	0.255	0.255
54	H	0.114	0.123	0.123	0.220	0.224	0.225
55	H	0.097	0.109	0.109	0.197	0.204	0.205
56	H	0.117	0.124	0.124	0.210	0.214	0.214

[a] See Ref. [15].
[b] See Refs. [16,17].

Table 3
Calculated molecular energies (E) and thermal enthalpies of carvedilol.

Medium	HF energy (E) Hartree/particle[a]	Solvent effect (ΔE) kJ/mol	Enthalpy ΔG kJ/mol
Vacuum (V)	−1340.618934		1291.0844
Water (W)	−1340.653573	−90.9455	1281.7875
DMSO (D)	−1340.651549	−85.6323	1280.0888
E(W)–E(D)		−5.3132	

[a] 1 Hartree/particle = 2625.5 kJ/mol.

large solvent effect of the polar solvents on the full molecule, since these kind of solvents repulse the electrons in the direction hydrogen atom to carbon atom. The result is that all C–H hydrogen atoms become more positive, and all carbon atoms become less positive or more negative.

Molecular energies

The calculated molecular energies and thermal enthalpies of CRV in different media are shown is Table 3.

Table 4
Selected internal coordinates and diagonal force constants of carvedilol.

Sl. No.	Internal coordinate[a,b,c]	Scale factor	Scaled diagonal force constants[d]		
			Isolated	In DMSO	In water
1	r (24,25)	0.955	6.412	6.392	6.396
2	r (25,27)	0.955	6.872	6.851	6.849
3	r (27,29)	0.955	6.783	6.736	6.732
4	r (29,28)	0.955	7.031	6.969	6.964
5	r (28,26)	0.955	6.734	6.687	6.683
6	r (26,24)	0.955	6.720	6.667	6.666
7	φ (24,28,26) $-\varphi$ (26,29,28) $+\varphi$ (28,27,29) $-\varphi$ (29,25,27) $+\varphi$ (27,24,25) $-\varphi$ (25,26,24)	1.079	1.895	1.873	1.874
8	2φ (24,28,26) $-\varphi$ (26,29,28) $-\varphi$ (28,27,29) $+\varphi$ (29,25,27) $-\varphi$ (27,24,25) $-\varphi$ (25,26,24)	1.079	8.223	8.092	8.087
9	φ (24,28,26) $-\varphi$ (26,29,28) $+\varphi$ (29,25,27) $-\varphi$ (27,24,25)	1.079	8.473	8.328	8.328
10	τ (24,26,28,29) $-\tau$ (26,28,29,27) $+\tau$ (28,29,27,25) $-\tau$ (29,27,25,24) $+\tau$ (27,25,24,26) $-\tau$ (25,24,26,28)	1.079	1.406	1.412	1.411
11	τ (24,26,28,29) $-\tau$ (28,29,27,25) $+\tau$ (27,25,24,26) $-\tau$ (29,27,25,24)	1.079	6.107	6.077	6.075
12	τ (24,26,28,29) -2τ (26,28,29,27) $+\tau$ (28,29,27,25) $+\tau$ (29,27,25,24) -2τ (27,25,24,26) $+\tau$ (25,24,26,28)	1.079	1.846	1.844	1.840
25	r (4,25)	0.661	4.107	3.995	3.989
26	φ (4,27,25)	1.285	2.902	2.870	2.866
28	r (30,4)	0.661	3.417	3.301	3.290
29	φ (30,25,4)	1.285	1.340	1.348	1.342
30	τ (30,4,25,27)	0.950	0.158	0.151	0.146
40	r (3,24)	0.661	4.742	4.719	4.706
41	φ (3,25,24)	1.285	3.450	3.382	3.404
43	r (23,3)	0.661	4.441	4.306	4.287
44	φ (23,24,3)	1.285	4.089	3.986	3.970
52	r (20,23)	0.769	3.448	3.453	3.445
53	φ (20,3,23)	0.948	1.418	1.386	1.400
61	r (6,20)	0.975	5.099	4.997	5.000
63[e]	τ (*6,20,23,3*)	0.858	0.104	0.081	0.106
64	r (41,6)	0.869	5.912	5.328	5.325
67	r (14,6)	0.975	5.066	4.935	4.942
68	φ (14,20,6)	0.878	1.085	1.080	1.092
69[e]	τ (*14,6,20,23*)	*0.858*	*0.065*	*0.086*	*0.106*
70	r (35,14)	0.905	4.250	4.313	4.320
76	r (12,14)	0.769	3.381	3.377	3.371
77	φ (12,6,14)	0.948	1.377	1.354	1.397
78[e]	τ (*12,14,6,20*)	*1.228*	*0.102*	*0.034*	*0.142*
82	r (2,12)	0.661	3.665	3.504	3.499
83	φ (2,14,12)	1.285	2.452	2.291	2.419
85	r (49,2)	0.782	*6.279*	*5.866*	*5.621*
88	r (13,12)	0.769	3.335	3.330	3.313
89	φ (13,14,12)	0.948	1.498	1.362	1.384
90[e]	τ (13,12,14,6)	1.228	1.836	1.839	1.874
103	r (17,11)	0.955	13.817	13.687	13.678
104	φ (17,1,11)	1.079	47.784	47.639	47.726
106	r (19,17)	0.955	8.940	8.834	8.833
107	φ (19,11,17)	1.079	46.784	46.475	46.473
109	r (15,19)	0.955	8.507	8.472	8.476
110	φ (15,17,19)	1.079	16.071	15.968	15.964
112	r (7,11)	0.955	9.083	8.958	8.952
113	φ (7,1,11)	1.079	47.184	47.154	47.196

(*continued on next page*)

Table 4 (*continued*)

Sl. No.	Internal coordinate[a,b,c]	Scale factor	Scaled diagonal force constants[d]		
			Isolated	In DMSO	In water
115	*r* (9,7)	0.955	26.184	25.928	25.931
116	*φ* (9,11,7)	1.079	16.488	16.466	16.507
127	*r* (5,9)	0.975	17.023	16.926	16.936
128	*φ* (5,7,9)	0.878	16.061	15.860	15.943
130	*r* (10,5)	0.975	16.797	16.818	16.825
131	*φ* (10,9,5)	0.878	33.042	32.829	32.874
133	*r* (8,10)	0.955	52.519	51.893	51.894
134	*φ* (8,5,10)	1.079	86.175	85.093	85.136
136	*r* (32,5)	0.805	6.061	5.121	5.103
139	*r* (18,10)	0.955	9.151	9.045	9.042
140	*φ* (18,8,10)	1.079	42.382	41.973	41.974
142	*r* (22,18)	0.955	8.822	8.751	8.753
143	*φ* (22,10,18)	1.079	14.708	14.578	14.574
145	*r* (16,8)	0.955	9.199	9.120	9.117
146	*φ* (16,7,8)	1.079	44.815	44.340	44.363
148	*r* (21,16)	0.955	8.248	8.201	8.197
149	*φ* (21,8,16)	1.079	16.015	15.837	15.840

[a] *r*: stretching; *φ*: in-plane bending; *γ*: out-of-plane bending; *τ*: torsion.
[b] For atom numbering of see Fig. 1.
[c] Large (relative) solvent effects in italics.
[d] For stretching coordinates in 10^2 N m^{-1}, for deformation ones in 10^{-18} N m units.
[e] Chain torsional coordinates.

Comparing the calculated molecular energies in different solvent, the conclusion is similar to those concluded for the solvent effect of the atomic net charges. The polar solvents stabilize the solute in comparison with the molecule in vacuum. However, the DMSO effect is smaller than that of the water, and the difference between the two solvent effects is essentially smaller than any of them. The order corresponds to the increasing dielectric constant of the medium.

The calculated thermal enthalpies are large. Their order is as follows: isolated molecule > solute in water > solute in DMSO. This order does not correspond to the order of the dielectric constant values. This is, however, in good correlation with the calculated dipole moments, namely for isolated molecule: 4.8042D, for solute in water: 6.3386D and for solute in DMSO: 6.4430D. That means, the order for the calculated dipole moments is isolated molecule < solute in water < solute in DMSO.

Vibrational force constants

The definitions of the vibrational internal coordinates of CRV are listed in Supplementary Table 4S together with corresponding scale factors and the scaled diagonal force constants of the isolated molecules and the solutes both in aqueous and DMSO solutions. Selected internal coordinates and diagonal force constants are shown in Table 4. Only diagonal force constants represent the force constant matrices regarding their large sizes ($162 \times 163/2$ independent force constants).

Looking at Table 4, at first glance several large force constants are significant. They belong to the coordinates 103, 104, 107, 110, 116, 134, 140, 146 and 149. One can find further ones in Table 4S, which are torsional and out-of-plane deformation coordinates. All these are coordinates of the carbazole part of the molecule. Similar deviations are not observed in the values of the geometric parameters (Table 1) and the atomic net charges (Table 2) of the carbazole part. These large force constants reflect large internal forces and therefore are the consequences of the choice of internal coordinates. The source of the problem is the method of the choice of the independent internal coordinates. It is easy to choose the six redundant internal coordinates for a six-membered ring. The definition of the 30 independent internal (symmetry) coordinates of benzene was given by Pulay et al. [26]. However, every molecule has six non-vibrational degrees of freedom. Therefore one cannot repeat this definition of internal (symmetry) coordinates since the molecule has two isolated aromatic systems. This is our case. The repetition of the benzene type coordinates was not possible. Therefore we had to use a less elegant definition for the internal coordinates of the carbazole system. Of course, in this case the reality of some force constants is dubious. For fused rings the definition of a butterfly coordinate is a solution [27]. However, this could not help in our problem.

We chose the phenyl group for eliminating the six redundant coordinates. Therefore the same method was not applicable for carbazole coordinates. The as-defined internal coordinates caused mechanical tensions. These were reflected in the high values of the force constants.

Comparing the corresponding diagonal force constants for the isolated molecule and for the solutes, respectively, the large differences are found between those of the isolated molecule and the solutes. Essentially smaller are the deviations between the corresponding values of the two solutes. Similar effects are observable comparing the similar geometric parameters (see Tables 1, 1S and 2, respectively).

The small effect of the solvents on the twisting of the chain connecting the phenyl and the carbazole groups is interesting (see Table 4).

Vibrational spectra

The measurements of the vibrational spectra are described in the *Methods and materials* section. Problems arose during the recording of infrared spectra of the solutions due to the very high absorption of the solvent. Similar problems arose with acquisition of the Raman spectra of the aqueous solution (owing to the fact that carvedilol is practically insoluble in water). The experimental spectra of solid CRV are presented in Figs. 2 together with the simulated spectra. In the infrared spectrum the NH stretching bands overlap with the OH stretching band and form a strong and broad band in the 3300–3100 cm^{-1} region, indicating the strong association with hydrogen bonds. The aliphatic CH stretching bands have here medium intensity, while the aromatic ones are of low intensity. In the Raman spectrum the NH stretching band has less intensity, while the aromatic CH stretching bands are intense. The

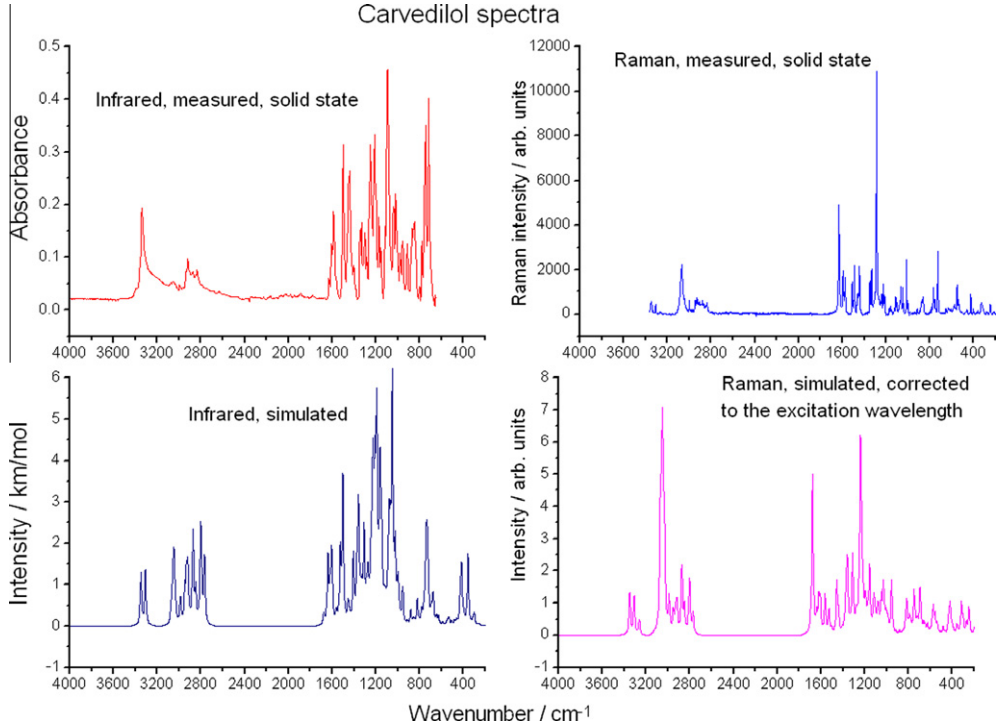

Fig. 2. Measured and simulated vibrational spectra of CRV.

comparison of the measured and simulated carvedilol spectra reflects the difference in the molecular states properly and the approaching character of the quantum chemical calculations as well. This difference is clearly observable in the infrared spectra in the 3400–2700 cm^{-1} region. However, at first sight the lower regions seem more similar. Since the Raman spectrum is less sensible to the associations, the measured and the simulated spectra are more similar. The calculations overestimate the intensities and of the overlapped CH stretching bands. See the very intense band between 3100 and 3000 cm^{-1} in comparison with the corresponding band in the measured spectrum.

The Raman spectrum of the CRV solute in DMSO is yielded by the subtraction of the solvent spectrum from the spectrum of the solution (we supposed low solute–solvent interaction). In Fig. 3 the solute spectrum shows only one negative band, indicating the particular overlapping of the CH stretching bands of the solute and the solvent in the solution. The solution CH band has a larger FWHH than the pure DMSO one and its maximum is shifted to the higher wavenumbers with about 1 cm^{-1}. The small band about 3070 cm^{-1} of the solution remains in the difference spectrum as well. The comparison of the spectrum of the measured CRV solute in DMSO and simulated CRV spectrum in "infinite" DMSO solvent seems similar below 1700 cm^{-1}. The bands over 2700 cm^{-1} are more intense in the simulated spectrum than in the measured one. The OH and NH stretching bands are not observable in the solute spectrum. The simulated CH stretching band is extremely intense in comparison with other strong bands in this spectrum, and also stronger, comparing with the similar band intensity ratios in the solute spectrum. The overestimated CH stretching band intensity occurs frequently in quantum chemically simulated Raman spectra.

The calculated Raman spectra are compared in Fig. 4. They look similar. Only the positions of the NH stretching bands are shifted to the lower wavenumbers in the order of CRV molecule → solute in DMSO → solute in water. Except for this difference the spectra of the two solutes do not show significant differences.

Fig 5 introduces the calculated infrared spectra of CRV and its solutes in DMSO and aqueous solutions, respectively. The most significant differences are seen between the spectra of the isolated molecule and the solute ones. One can compare the spectral regions over 2750 cm^{-1}. The shift of the NH stretching bands is also here important, in the same sense as in case of the of Raman spectra.

The results of PED calculations for CRV, solutes in DMSO and water are given in Tables 5–7, respectively. The solvent effect on calculated vibrational modes, results of the PCM calculations and the scaling are analyzed below.

The OH, NH and CH stretching motions build true group frequencies.

The OH stretching vibration (of the O2–H49 bond) on the chain shows strong medium effect. While calculated frequency for this vibration of isolated molecule is 3349.5 cm^{-1}, the corresponding values are 3328.1 cm^{-1} in DMSO solution and 3169.0 cm^{-1} in aqueous solution.

The corresponding values for the chain NH group (N6–H41) are 3261.7, 3099.7 and 3098.7 cm^{-1}, while they are for the carbazole NH group (N5–H32) 3308.8, 3046.7, 3041.4 cm^{-1}. The solvent effects are strong for all these group frequencies and follow the increasing values of the dipole moment. Besides, the solvents affect stronger on the carbazole NH stretching mode than on the chain one, the frequency order is changed.

The solvent effect polarizes the OH and NH bonds (see Table 2 for the atomic net charges). However, there is a difference in the polarization of the two NH bonds. For the N6–H41 bond the nitrogen atom becomes more negative, the hydrogen atom more positive under the solvent effect, while for the N5–H32 bond the net charge of the nitrogen atom remains practically constant, only its hydrogen atom charge changes in the positive direction. The difference in the two NH bond polarizations is reflected in the different NH stretching frequencies. Similarly, one can follow the changes in the diagonal force constants (Table 4), the drift of internal coordinates 85 (O2–H49), 64 (N6–H41) and 136 (N5–H32). Furthermore,

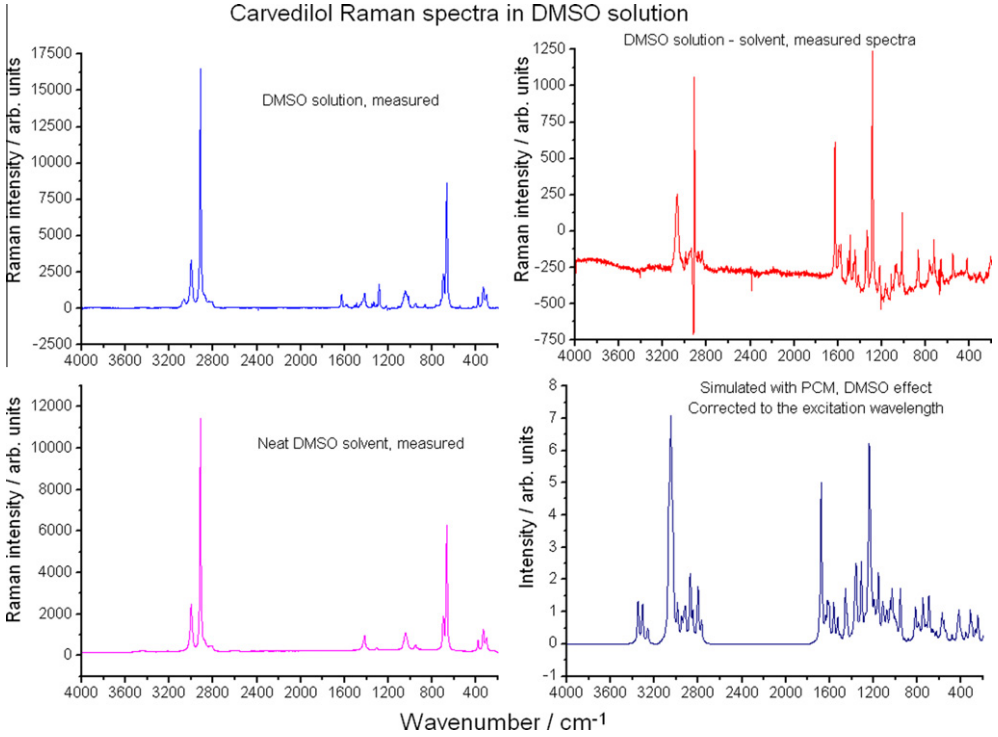

Fig. 3. DMSO effect on CRV, comparison of measured and simulated Raman spectra.

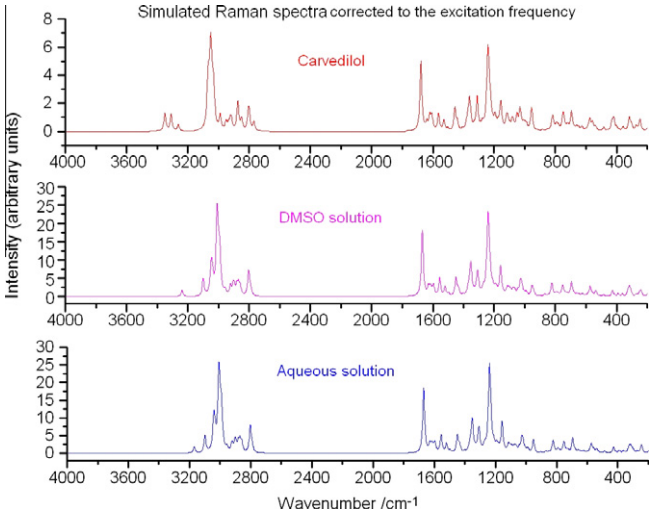

Fig. 4. Simulated Raman spectra of the CRV molecule and the solute in solutions.

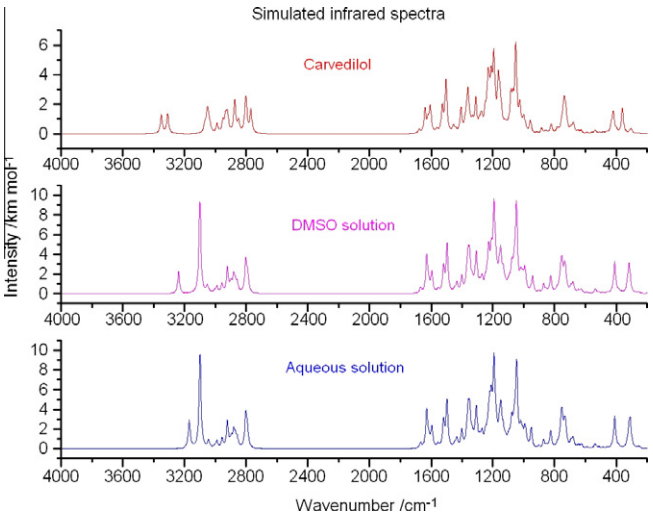

Fig. 5. Simulated infrared spectra of the CRV molecule and the solutes.

the bond lengths show this effect as well. All the mentioned bonds increase due to the solvent effects (Table 1).

Some of CH stretching modes are coupled, i.e. more than one CH groups move in these normal modes. We marked those belonging to the lower ring in Fig. 1 as carbazole A, and those of the higher ring as carbazole B; chain A contains those on the left part of the chain between the carbazole and phenyl groups, with chain B contains those on its right part. The CH stretching motions of the five parts of the molecule, namely carbazole A, carbazole B, chain A, chain B and phenyl do not mix.

Some individual CH group frequencies exist. The carbazole C17–H39 frequency belongs to a bond very close to the C11–O1 bond (Fig. 1) and feels its electron effect. However, the appearance of the C16–H38 group frequency under the solvent effect may be caused by the large changes in their atomic net charges. One individual phenyl group frequency was observed under the solvent effect, C26–H50. The change in this bond length is negligible, only the electron effect can explain this effect. Three chain CH normal modes were found individual, C12–H31, C20–H44 and C14–H35. The first one has common carbon atom with the chain C–OH group, the two other are on vicinal carbon atoms to the chain NH group. Therefore each feels the strong electron effect of the OH and NH groups, respectively (Table 2). Their solvent effect is negligible. The individual C12–H36 group frequency is the result of the solvent effect (Figs. 4 and 5).

Table 5
Properties of vibrational modes of the carvedilol molecule.

Frequency (cm^{-1})[a]		Potential energy distribution[b] (%)			
Measured	Calculated				
3348.9	3349.5	νOH 99	Chain OH		
3309.7	3308.8	νNH 99	Carbazole NH		
3261.7	3261.7	νNH 99	Chain NH		
3076.9	3071.3	νCH 99	Carbazole C17–H39		
3067.8	3067.9	νCH 99	Phenyl CH coupled		
3058.0	3062.9	νCH 99	Carbazole CH B coupled[c]		
3058.0	3055.3	νCH 99	Phenyl CH coupled		
3041.4	3049.8	νCH 96	Carbazole CH A coupled[c]		
3041.4	3048.8	νCH 96	Carbazole CH B coupled[c]		
3041.4	3043.4	νCH 99	Phenyl CH coupled		
3034.4	3036.4	νCH 99	Carbazole CH B coupled[c]		
3034.4	3032.4	νCH 99	Carbazole CH A coupled[c]		
3034.4	3030.6	νCH 99	Phenyl CH coupled		
3017.4	3026.1	νCH 99	Carbazole CH B coupled[c]		
2991.1	2988.9	νCH 99	Methyl CH coupled		
2944.3	2950.1	νCH 99	Methyl CH coupled		
2928.9	2933.9	νCH 97	Chain CH A coupled[c]		
2928.9	2922.9	νCH 99	Chain CH B coupled[c]		
2923.1	2917.0	νCH 97	Chain CH A coupled[c]		
2923.1	2914.1	νCH 99	Chain CH B coupled[c]		
2870.4	2875.4	νCH 99	Methyl CH coupled		
2870.4	2871.5	νCH 99	Chain CH B coupled[c]		
2850.1	2849.0	νCH 98	Chain CH A coupled[c]		
2797.8	2805.8	νCH 99	Chain C12–H31		
2797.8	2800.2	νCH 99	Chain C20–H44		
2775.8	2768.8	νCH 99	Chain C14–H35		
1632.1	1677.7	νrg 28	βrg 52		
1632.1	1640.2	νrg 41	βrg 28	νNC 11	
1607.7	1621.0	νrg 70	βrg 10	βCO 12	
1597.5	1612.8	νrg 73	βrg 11	βCH 11	
1587.5	1606.0	νrg	59 βrg 23		
1575.3	1563.3	νrg 30	βrg 27	βCH 14	νNC 15
1510.0	1528.3	νrg 35	βrg 42		
1502.5	1505.1	νrg 34	β rg 31	βCH 10	
1490.0	1502.2	βNH 82			
1470.4	1456.6	νrg 44	βCH 39		
1453.3	1454.6	νrg 32	βrg 22	βCH	29
1453.3	1440.5	νrg 47	βCH 30	βCO 12	
1445.0	1440.2	νrg 41	βCH 14	νNC 12	βNH 12
1403.8	1407.1	νrg 64	βCH 10		
1403.8	1384.1	βCH 44	γCH 50		
1383.6	1378.8	βCH 52	γCH 43		
1383.6	1371.7	βCH 13	γCH 74		
1348.7	1364.5	βCH 53	γCH 37		
1348.7	1360.7	βCH 25	γCH 60		
1348.7	1356.7	νrg 53	βCH 13	γCH 14	
1348.7	1354.0	γCH 82			
1348.7	1349.3	βCH 18	γCH 80		
1334.0	1338.9	βCH 34	γCH 41		
1334.0	1331.0	βCH 69	γCH 10		
1334.0	1328.8	νrg 55	βCH 12		
1304.0	1312.3	νrg 44	βCH 27	γCH 19	
1304.0	1310.3	νrg 32	βCH 31	γCH 23	
1283.5	1289.5	νrg 21	βCH 28	νNC 28	
1253.4	1278.3	βrg 22	βCH 48	βNC 11	
1249.8	1270.7	βCH 43	γCH 31		
1249.8	1250.4	βCH 74	γCH 15		
1249.8	1241.5	νrg 13	βrg 18	νNC 24	βNH 22
1236.9	1233.2	βCH 75			
1225.7	1231.3	βCH 84			
1215.0	1221.8	βCH 80			
1215.0	1209.9	βCH 67	γCH 21		
1200.4	1195.4	βCH 45	βCH 13		
1200.4	1187.6	νrg 18	βrg 21	βCH 47	
1175.5	1175.4	βCH 55			
1169.9	1164.5	βCH 50	γCH 13	βOH 20	
1156.1	1155.6	νrg 24	βrg 18	βCH 17	νCO 35
1146.4	1147.1	βCH 11	νNC 80		
1146.4	1145.3	νrg 10	βrg 35	βCH 22	νCO 24
1125.2	1126.7	βCH 60	γCH 17		
1118.6	1119.4	βCH 65	γCH 15		
1111.4	1112.7	νrg 19	βCH 73		
1111.4	1112.0	νrg 17	βCH 66		

(*continued on next page*)

Table 5 (*continued*)

Frequency (cm^{-1})[a]		Potential energy distribution[b] (%)					
Measured	Calculated						
1102.3	1103.3	νrg 17	βrg 11	βCH 59			
1094.9	1097.3	βCH 24	γCH 18	βCC 10	νNC 14		
1094.9	1083.8	νrg 21	βrg 12	βCH 54			
1094.9	1081.4	βCH 80	γCH 17				
1064.9	1075.1	νrg 22	βCH 65				
1064.9	1070.2	νrg 14	βrg 21	βCH 54			
1047.6	1051.9	γCH 44	νCO 12				
1047.6	1049.8	νrg 34	βrg 14	βCH 34			
1047.6	1032.3	νrg 25	βrg 55				
1020.1	1027.2	νrg 15	βCH 15	γCH 29	νCC 10		
1013.8	1024.8	νrg 43	βCH 35	γCH 11			
1009.1	1008.6	βCH 16	γCH 15	νCC 28	βCC 10		
1001.7	999.7	νrg 18	νCO 17	νNC 16			
979.3	989.0	νCC 24	νNC 34				
979.3	956.8	τrg 59					
956.6	954.8	τrg 20	γCH 14	νCC 15	βOH 12		
914.3	916.0	νCO 77					
878.9	884.2	νrg 11	νCO 75				
878.9	881.0	νCO 26	βCO 24	τCO 22			
862.8	868.4	νrg 32	βrg 24	νNC 12	βNC 13		
862.8	863.3	γCH 98					
849.2	853.2	γCH 32	βCO 10	νCC 25			
849.2	840.6	νCH 93					
801.2	823.6	γCH 90					
801.2	821.9	γCH 77					
801.2	815.7	γCH 86					
797.8	795.9	νrg 13	βrg 20	νCO 30			
784.4	792.5	νrg 15	βrg 15	γCH 13	νCO 30		
781.0	782.8	τrg 28	γCH 38				
781.0	780.5	τrg 55	γCH 39				
769.4	768.5	νrg 13	βrg 11	γCH 12	νCO 30		
754.9	759.3	γCH 74					
749.2	752.3	τrg 12	γCH 84				
744.4	748.8	τrg 11	γCH 80				
744.4	740.6	νrg 10	βrg 12	τrg 22	γCH 10	νCO 15	γNH 12
727.1	735.6	γCH 57					
720.4	726.9	νrg 30	βrg 20	νCO 17			
717.5	717.9	γCH 25	γNH 52				
717.5	695.1	γCH 73	τCO 10				
669.8	686.0	τrg 10	νCH 81				
669.8	677.7	τrg 12	γCH 76				
654.8	662.0	νrg 20	βrg 41	βNC 10			
654.8	648.0	νrg 16	βrg 33	βNC 35			
633.2	630.7	τrg 83					
622.4	626.5	νrg 14	βrg 42	βCO 14			
609.6	606.4	τrg 77	τNC 15				
609.6	604.2	βrg 23	τrg 25	γCH 12	βCO 11		
588.3	591.1	νrg 10	βrg 29	βCO 18	βNC 12		
575.0	583.0	βrg 27	βCO 20	βNC 12			
575.0	575.0	νrg 10	βrg 75				
549.7	557.9	τrg 75	τNC 15				
539.1	540.5	βrg 15	νCO 14	βCO 24			
530.7	531.2	τrg 27	βCO 18	τCO 14			
509.4	509.1	γCH 14	βCO 10	τCO 24	τCC 14		
509.4	485.4	τrg 46	νCO 13				
509.4	484.5	τrg 73					
426.0	464.4	βrg 13	βCO 20	βCC 10	βNC 18		
426.0	430.9	νrg 10	βrg 19	βCO 14	νNC 13	βNC 16	γOH 13
403.1	418.9	νrg 13	βrg 14	νNC 11	γOH 31		
403.1	401.4	βrg 11	βCO 15	γOH 43			
403.1	389.8	τrg 33	βCO 26	βNC 11			
362.5	360.0	βrg 13	τrg 20	νCO 10	βCO 19	βNC 10	
349.7	356.9	τrg 32	γNH 63				
328.5	318.4	βrg 24	βCO 21	βCC 19	τCC 10		
313.3	309.7	τrg 45	τNC 45				
313.3	301.6	τrg 63	τNC 12	γNH 21			
278.8	272.5	βrg 17	βCO 25	τCO 22	βCC 13	βNC 10	
246.7	259.3	βrg 12	νCO 26	βCO 20	νCC 10		
246.7	249.6	βCO 23	τCO 33				
246.7	246.9	τrg 87					
190.4	194.5	βrg 21	βCO 23	βNC 27			
171.0	169.5	τrg 29	τCO 26	τNC 27			
170.7	164.8	τrg 22	γCH 25	τCO 23			
159.7	153.8	γCH 14	τCO 33	τNC 40			

Table 5 (*continued*)

Frequency (cm^{-1})[a]		Potential energy distribution[b] (%)				
Measured	Calculated					
146.7	142.8	τrg 11	γCH 32	τCO 20	τNC 19	
134.2	132.9	τrg 21	τCO 13	τCC 15	τNC 30	
116.7	113.2	βCO 21	βCC 20			
110.7	109.2	τrg 33	τCO 10	τNC 27		
107.3	104.4	βCO 12	τCO 18	βCC 10	βNC 12	τNC 12
101.6	98.2	τCO 42	τCC 13	τNC 15		
94.4	90.5	τCO 12	τNC 59			
83.6	80.9	τCO 70				
55.8	57.6	τCO 22	τCC 45	τNC 11		
48.1	48.2	βrg 13	βCO 14	τCO 15	τCC 12	τNC 15
45.3	45.8	βCO 11	τCO 29	βCC 12	βNC 11	τNC 21
27.7	27.9	τrg 18	τCO 40	τCC 18	τNC 21	
16.3	16.3	βCO 10	βCC 44	βNC 36		
12.1	12.3	τrg 29	τCO 19	τCC 28	τNC 21	
10.5	10.6	τCO 12	τCC 42	τNC 44		

Mean difference: 6.65 cm^{-1}.
Mean rel. difference: 1.00%.
[a] Frequencies below 200 cm^{-1} are taken from the calculated ones.
[b] Distributions not less than 10%; ν: stretching; β: in-plane deformation; γ: out-of-plane deformation;τ: torsion; rg: benzene ring.
[c] carbazole A: CH's for H37 and H42; carbazole B: CH's for H38, H40, H46 and H38; chain A: CH's for H33, H34 and H36; chain B: CH's for H43, H47 and H48; for atom numbering see Fig. 1.

Table 6
Properties of vibrational modes of the carvedilol molecule in DMSO solution.

Frequency (cm^{-1})		Potential energy distributions (%)[a]				
Measured	Calculated					
–	3238.1	νOH 99	Chain OH			
3070.6	3099.7	νNH 99	Chain NH			
3070.6	3053.7	νCH 99	Carbazole C16–H38			
3070.6	3046.7	νNH 95	Carbazole NH			
3070.6	3044.8	νCH 96	Carbazole C17–H39			
–	3037.8	νCH 99	Phenyl C26–H50			
–	3011.4	νCH 99	Phenyl CH coupled[b]			
–	3009.5	νCH 98	Carbazole CH A coupled[b]			
–	3007.6	νCH 98	Carbazole CH B coupled[b]			
–	3000.0	νCH 99	Phenyl CH coupled[b]			
–	2997.5	νCH 99	Carbazole CH B coupled[b]			
–	2992.7	νCH 99	Carbazole CH A coupled[b]			
–	2992.1	νCH 99	Phenyl CH coupled[b]			
–	2990.0	νCH 99	Methyl CH coupled[b]			
–	2987.5	νCH 99	Carbazole CH B coupled[b]			
–	2957.0	νCH 99	Methyl CH coupled[b]			
–	2922.2	νCH 99	Chain CH A coupled[b]			
–	2921.8	νCH 96	Chain CH B coupled[b]			
–	2903.1	νCH 98	Chain CH B coupled[b]			
–	2896.7	νCH 99	Chain C14–H36			
–	2880.7	νCH 99	Methyl CH coupled[b]			
–	2870.4	νCH 99	Chain CH A coupled[b]			
–	2857.7	νCH 99	Chain CH B coupled[b]			
–	2803.8	νCH 99	Chain C12–H31			
–	2802.4	νCH 99	Chain C20–H44			
–	2790.0	νCH 99	Chain C14–H35			
1628.8	1669.2	νrg 28	βrg 52			
1628.8	1629.4	νrg 42	βrg 29	νNC 10		
1590.7	1615.5	νrg 70	βrg 10	βCO 12		
1590.7	1606.8	νrg 73	βrg 11	βCH 10		
1575.3	1596.2	νrg 58	βrg 24			
–	1555.2	νrg 30	βrg 27	βCH 13	νNC	16
1512.0	1520.4	νrg 36	βrg 42			
1491.7	1497.3	νrg 19	βrg 16	βNH 42		
–	1496.8	νrg 16	βrg 13	βNH 49		
1459.5	1449.5	νrg 44	βCH 39			
1444.6	1448.2	νrg 32	βrg 25	βCH 29		
–	1434.2	νrg 48	βCH 33	βCO 13		
–	1430.3	νrg 39	βCH 13	νNC	13	βNH 14
–	1402.3	νrg 65				
–	1376.2	βCH 40	γCH 55			
–	1372.9	βCH 62	γCH 33			

(*continued on next page*)

Table 6 (*continued*)

Frequency (cm^{-1})		Potential energy distributions (%)[a]				
Measured	Calculated					
–	1365.9	βCH 21	γCH 69			
1351.2	1360.5	βCH 48	γCH 42			
1351.2	1354.5	νrg 13	βCH 29	γCH 48		
–	1351.6	νrg 47	βCH 15	γCH 23		
1336.4	1347.1	γCH 80				
1336.4	1344.3	βCH 18	γCH 80			
1336.4	1335.2	βCH 44	γCH 30			
–	1330.7	βCH 60	γCH 18			
–	1322.6	νrg 53	βCH 11	νNC	11	
–	1312.3	βCH 51	γCH 23			
–	1306.2	νrg 62	γCH 30			
1286.4	1285.5	νrg 22	βCH 15	βCH 14	νNC 28	
1286.4	1273.9	βrg 22	βCH 48	βNC 10		
–	1268.7	βCH 42	γCH 29			
–	1249.8	βCH 79	γCH 11			
–	1239.6	νrg 12	βrg 17	βCH 13	νNC 23	βNH 23
–	1230.7	βCH 81				
–	1228.5	βCH 73				
–	1220.5	βCH 83				
–	1209.2	βCH 70	γCH 17			
–	1193.2	βCH 48				
–	1182.9	νrg 20	βrg 18	βCH 39		
–	1173.1	βCH 58	γCH 10			
–	1157.6	βCH 51	γCH 13	βOH 15		
–	1148.5	νrg 20	βrg 27	βCH 15	νCO 33	
–	1136.2	νrg 10	βrg 19	βCH 34	γCH 10	νCO 20
–	1132.1	νNC	84			
1114.5	1121.6	βrg 16	βCH 49	γCH 12		
1114.5	1113.2	βCH 45	γCH 20			
1114.5	1102.7	νrg 20	βCH 73			
–	1101.0	νrg 17	βCH 61			
–	1093.0	νrg 15	βrg 12	βCH 52		
–	1089.6	βCH 25	βCH 11	γCH 12	νNC 10	
–	1077.5	βCH 80	γCH 17			
–	1075.6	νrg 16	βrg 22	βCH 52		
–	1066.7	νrg 20	βCH 68			
–	1062.1	νrg 19	βCH 64			
1050.1	1047.7	γCH 54	□			
1050.1	1043.0	νrg 33	βrg 18	βCH 24	βCH 14	
–	1028.0	νrg 28	βrg 55			
1015.7	1020.8	νrg 52	βCH 34			
1015.7	1018.5	βCH 14	γCH 44			
–	1007.5	βCH 16	νCC 34		βCC 12	
–	993.9	νrg 12	νCO 10	νCC 20	νNC 24	
–	985.8	νrg 13	νCO 14	νCC 13	νNC 25	
–	953.1	τrg 62				
–	941.7	γCH 17	βCO 11	νCC 18	βOH 29	
–	902.5	νCO 76				
868.3	871.3	νCO 26	βCO 18	τCO 17		
868.3	870.7	γCH 35	νCO 35			
868.3	868.3	γCH 57	νCO 30			
868.3	864.7	νrg 23	βrg 14	νCO 12	βCO 11	τCO 10
849.2	853.7	γCH 32	νCC 30			
–	840.0	νCH 89				
–	830.9	γCH 88				
–	824.5	γCH 79				
–	822.3	γCH 87				
–	797.4	νrg 13	βrg 10	νCO 24	γNH 20	
–	792.4	βrg 12	τrg 14	γCH 24	νCO 19	
–	783.9	τrg 54	γCH 40			
–	781.9	νrg 11	βrg 10	τrg 17	γCH 20	νCO 18
769.0	770.7	νrg 12	βrg 12	γCH 18	νCO 13	γNH 15
–	760.5	γCH 42	νCO 27	γNH 10		
749.3	756.9	γCH 86				
749.3	753.4	τrg 20	γCH 51	γNH 15		
749.3	751.0	τrg 22	γCH 67			
722.6	736.6	γCH 53				
722.6	730.9	νrg 11	βrg 10	τrg 13	γCH 32	νCO 12
722.6	722.4	νrg 30	βrg 20	νCO 19		
–	694.7	γCH 72	τCO 10			
–	687.4	τrg 10	γCH 88			
–	679.0	τrg 14	γCH 75			
–	660.5	νrg 21	βrg 40	βNC 10		
–	646.1	νrg 15	βrg 30	βNC 33		

Table 6 (*continued*)

Frequency (cm^{-1})		Potential energy distributions (%)[a]				
Measured	Calculated					
–	631.1	τrg 68				
–	624.3	νrg 12	βrg 40	τrg 12	βCO 13	
–	607.6	τrg 75	τNC 14			
–	604.9	βrg 20	τrg 32	γCH 12	βCO 10	
–	591.2	νrg 11	βrg 26	βCO 21	βNC	10
–	582.2	βrg 32	βCO 18	βNC 14		
–	573.0	νrg 10	βrg 75			
551.1	559.4	τrg 74	τNC 16			
–	537.2	βrg 14	νCO 15	βCO 22		
–	529.0	βrg 10	τrg 25	βCO 17	τCO 14	
–	512.3	γCH 12	βCO 10	τCO 24	τCC 13	
–	486.8	βrg 13	τrg 31	νCO 20	βCO 11	τCO 11
–	485.0	τrg 82				
–	461.3	βrg 10	βCO 20	βCC 11	βNC 18	
424.2	427.0	νrg 15	βrg 28	βCO 10	νNC 19	βNC 19
–	409.6	νrg 12	βrg 14	βCO 29	βCC 11	
–	391.3	τrg 30	βCO 23	βNC 12		
–	381.7	τrg 11	γNH 87			
–	363.2	βrg 14	τrg 22	νCO 12	βCO 17	βNC 11
–	326.4	βrg 18	βCO 16	βCC	16	γOH 11
–	317.4	τrg 85				
–	309.5	τrg 15	τNC 17	γOH 53		
–	306.5	τrg 19	τNC 37	γOH 24		
–	271.6	βrg 13	βCO 24	τCO 15	βCC 12	βNC 11
–	252.8	βrg 12	νCO 24	βCO 23	νCC 10	
–	250.2	τrg 16	βCO 16	τCO 40		
–	241.9	τrg 72				
–	198.6	βrg 22	βCO 24	βNC 27		
–	165.9	τrg 14	γCH 16	τCO 23	τCC 13	τNC 13
–	161.3	τCO 26	τCC 12		τNC 40	
–	150.8	τrg 16	γCH 15	τCO 14	τNC 31	
–	143.6	τrg 18	γCH 35	τCO 19	τNC 20	
–	132.1	τrg 17	τCO 14	τCC 14	τNC 39	
–	120.3	βCO 10	τCO 44	βCC 11		
–	114.0	νCO 11	βCO 14	τCO 19	νCC 12	βCC 10
–	105.5	τrg 12	τCO 12	τNC 27		
–	104.0	τrg 21	βCO 13	τCO 19	τNC 13	
–	90.8	τCO 17	τNC 55			
–	82.6	τCO 70	τNC 14			
–	67.1	τrg 15	τCO 26	τCC 42	τNC 11	
–	51.2	βrg 21	βCO 21	τCO 15	βCC 15	βNC 13
–	43.6	τCO 37	τNC 24			
–	32.4	τrg 27	τCO 31	τCC 16	τNC 23	
–	18.0	τCO 22	τCC 29	τNC 45		
–	13.3	βCO 11	βCC 44	βNC 33		
–	17.6[c]	τCO 17	τCC 52	τNC 18		

[a] *ν*: stretching; *β*: in-plane deformation; *γ*: out-of-plane deformation;*τ*: torsion; rg: ring; distributions not less than 10%;*ν*:stretching; *β*:in-plane deformation; *γ*: out-of-plane deformation;*τ*: torsion; rg: benzene ring.

[b] carbazole A: CH's for H37 and H42; carbazole B: CH's for H40, H46 and H38; chain A: CH's for H33 and H34; chain B: CH's for H43, H47 and H48; for atom numbering see Fig. 1.

[c] Imaginary frequency (absolute value).

Table 7
Properties of vibrational modes of the carvedilol molecule in aqueous solution.

Frequency (cm^{-1})		Potential energy distribution[b] (%)	
Measured[a]	Calculated		
3348.9	3169.0	νOH 99	Chain OH
3309.7	3098.7	νNH 99	Chain NH
3261.7	3044.7	νCH 98	Carbazole C16–H38
3076.9	3041.4	νNH 90	Carbazole NH
3067.8	3040.2	νCH 92	Carbazole C17–H39
3058.0	3032.1	νCH 99	Phenyl C26–H50
3058.0	3010.3	νCH 99	Phenyl CH coupled
3041.4	3009.0	νCH 99	Carbazole CH A coupled[c]
3041.4	3006.7	νCH 98	Carbazole CH B coupled[c]
3041.4	2998.5	νCH 99	Phenyl CH coupled
3034.4	2996.7	νCH 99	Carbazole CH B coupled[c]
3034.4	2991.8	νCH 99	Carbazole CH A coupled[c]

(*continued on next page*)

Table 7 (*continued*)

Frequency (cm^{-1})		Potential energy distribution[b] (%)				
Measured[a]	Calculated					
3034.4	2991.0	*v*CH 99	Phenyl CH coupled			
3017.4	2989.7	*v*CH 99	Methyl CH coupled			
2991.1	2986.8	*v*CH 99	Carbazole CH B coupled[c]			
2944.3	2956.5	*v*CH 99	Methyl CH coupled			
2928.9	2922.0	*v*CH 99	Chain CH A coupled[c]			
2928.9	2921.7	*v*CH 96	Chain CH B coupled[c]			
2923.1	2902.7	*v*CH 98	Chain CH B coupled[c]			
2923.1	2895.8	*v*CH 99	Chain C14–H36			
2870.4	2880.7	*v*CH 99	Methyl CH coupled			
2870.4	2870.2	*v*CH 99	Chain CH A coupled[c]			
2850.1	2857.7	*v*CH 99	Chain CH B coupled[c]			
2797.8	2802.9	*v*CH 99	Chain C12–H31			
2797.8	2802.0	*v*CH 99	Chain C20–H44			
2775.8	2792.3	*v*CH 99	Chain C14–H35			
1632.1	1668.6	*v*rg 28	*β*rg 52			
1632.1	1628.7	*v*rg 41	*β*rg 29	*v*NC 10		
1607.7	1615.2	*v*rg 70	*β*rg 10	*β*CO 12		
1597.5	1606.4	*v*rg 73	*β*rg 11	*β*CH 10		
1587.5	1595.5	*v*rg 58	*β*rg 24			
1575.3	1555.1	*v*rg 29	*β*rg 28	*β*CH 13	*v*NC 16	
1510.0	1519.8	*v*rg 36	*β*rg 42			
1502.5	1498.7	*β*NH 84				
1490.0	1496.5	*v*rg 36	*β*rg 30	*β*CH 10		
1470.4	1449.0	*v*rg 44	*β*CH 39			
1453.3	1447.9	*v*rg 32	*β*rg 25	*β*CH 29		
1453.3	1433.8	*v*rg 48	*β*CH 33	*β*CO 13		
1445.0	1429.3	*v*rg 40	*β*CH 13	*v*NC 13	*β*NH 14	
1403.8	1402.0	*v*rg 65				
1403.8	1375.7	*β*CH 38	*γ*CH 57			
1383.6	1373.0	*β*CH 65	*γ*CH 30			
1383.6	1365.3	*β*CH 21	*γ*CH 69			
1348.7	1360.3	*β*CH 46	*γ*CH 44			
1348.7	1354.1	*v*rg 12	*β*CH 28	*γ*CH 51		
1348.7	1351.2	*v*rg 50	*β*CH 15	*γ*CH 19		
1348.7	1346.1	*γ*CH 82				
1348.7	1344.3	*β*CH 18	*γ*CH 80			
1334.0	1334.1	*β*CH 46	*γ*CH 28			
1334.0	1330.1	*β*CH 60	*γ*CH 18			
1334.0	1322.3	*v*rg 52	*β*CH 11	*v*NC 12		
1304.0	1311.8	*β*CH 50	*γ*CH 24			
1304.0	1305.8	*v*rg 62	*γ*CH 30			
1283.5	1285.6	*v*rg 22	*β*CH 29	*v*NC 28		
1253.4	1274.0	*β*rg 20	*β*CH 49	*β*NC 10		
1249.8	1269.1	*β*CH 36	*γ*CH 30			
1249.8	1249.5	*β*CH 80	*γ*CH 10			
1249.8	1238.8	*v*rg 11	*β*rg 17	*β*CH 15	*v*NC 22	*β*NH 23
1236.9	1230.4	*β*CH 79				
1225.7	1228.3	*β*CH 73				
1215.0	1220.6	*β*CH 82				
1215.0	1210.1	*β*CH 72	*γ*CH 16			
1200.4	1193.0	*β*rg 10	*β*CH 49			
1200.4	1182.5	*v*rg 21	*β*rg 17	*β*CH 39		
1175.5	1174.5	*β*CH 58				
1169.9	1157.1	*β*CH 50	*γ*CH 19	*β*OH 14		
1156.1	1148.0	*v*rg 20	*β*rg 27	*β*CH 15	*v*CO 33	
1146.4	1135.8	*v*rg 10	*β*rg 19	*β*CH 34	*γ*CH 10	*v*CO 20
1146.4	1133.5	*v*NC 84				
1125.2	1121.3	*β*rg 16	*β*CH 48	*γ*CH 12		
1118.6	1114.1	*β*CH 49	*γ*CH 20			
1111.4	1102.7	*v*rg 20	*β*CH 73			
1111.4	1100.6	*v*rg 17	*β*CH 63			
1102.3	1093.3	*v*rg 15	*β*rg 13	*β*CH 54		
1094.9	1089.4	*β*CH 25	*γ*CH 11	*v*NC 11	*β*OH 10	
1094.9	1077.7	*β*CH 80	*γ*CH 17			
1094.9	1075.8	*v*rg 15	*β*rg 24	*β*CH 11	*β*CH 39	
1064.9	1066.3	*v*rg 21	*β*CH 67			
1064.9	1062.1	*v*rg 20	*β*CH 12	*β*CH 54		
1047.6	1046.8	*γ*CH 53				
1047.6	1043.1	*v*rg 32	*β*rg 19	*β*CH 24	*β*CH 15	
1047.6	1027.7	*v*rg 28	*β*rg 55			
1020.1	1020.2	*v*rg 51	*β*CH 34			

Table 7 (*continued*)

Frequency (cm^{-1})		Potential energy distribution[b] (%)				
Measured[a]	Calculated					
1013.8	1018.6	βCH 15	γCH 47			
1009.1	1006.8	βCH 14	νCC 37	βCC 13		
1001.7	992.8	νrg 14	νCO 12	νCC 16	νNC 23	
979.3	984.5	νrg 11	νCO 12	νCC 16	νNC 27	
979.3	952.3	τrg 61				
956.6	951.4	γCH 18	βCO 11	νCC 18	βOH 24	
914.3	902.6	νCO 76				
878.9	871.1	νCO 23	βCO 21	τCO 19		
878.9	870.4	γCH 62	νCO 24			
862.8	867.9	γCH 35	νCO 48			
862.8	864.8	νrg 23	βrg 14	νCO 13	βCO 12	τCO 11
849.2	852.0	γCH 34	νCC 32			
849.2	839.2	νCH 88				
801.2	831.0	γCH 89				
801.2	824.6	γCH 79				
801.2	822.3	γCH 87				
797.8	795.9	νrg 12	βrg 12	νCO 25	γ	NH 16
784.4	791.8	βrg 10	τrg 14	γCH 23	νCO 19	
781.0	783.8	τrg 55	γCH 10	νCH 29		
781.0	781.4	νrg 10	βrg 10	τrg 17	γCH 21	νCO 18
769.4	769.9	νrg 12	βrg 12	γCH 18	νCO 16	γ NH 13
754.9	759.4	γCH 51	νCO 21			
749.2	756.6	γCH 84				
744.4	751.9	τrg 22	γCH 40	γNH 18		
744.4	750.5	τrg 21	γCH 62			
727.1	736.6	γCH 53				
720.4	730.3	νrg 11	βrg 10	τrg 12	γCH 32	νCO 11
717.5	722.5	νrg 30	βrg 20	νCO 19		
717.5	694.7	γCH 72				
669.8	687.5	τrg 10	γCH 88			
669.8	678.7	τrg 14	γCH 76			
654.8	660.3	νrg 21	βrg 40	βNC 10		
654.8	646.3	νrg 16	βrg 31	βNC 34		
633.2	631.1	τrg 73				
622.4	624.0	νrg 13	βrg 41	τrg 10	βCO 13	
609.6	607.2	τrg 75	τNC 14			
609.6	604.8	βrg 20	τrg 32	γCH 12	βCO 10	
588.3	591.4	νrg 11	βrg 26	βCO 21	βNC 10	
575.0	582.2	βrg 31	βCO 18	βNC 14		
575.0	572.9	νrg 10	βrg 75			
549.7	559.2	τrg 74	τNC 15			
539.1	539.1	βrg 15	νCO 15	βCO 23		
530.7	529.3	βrg 10	τrg 27	βCO 17	τCO 14	
509.4	512.5	γCH 12	βCO 10	τCO 24	τCC 13	
509.4	485.8	βrg 11	τrg 38	ννCO 17	τCO 10	
509.4	485.1	τrg 79				
426.0	461.6	βCO 21	βCC 11	βNC 18		
426.0	427.9	νrg 14	βrg 27	βCO 12	νNC 18	βNC 19
403.1	410.1	νrg 13	βrg 15	βCO 28	βCC 11	
403.1	391.1	τrg 30	βCO 23	βNC 12		
403.1	383.8	τrg 11	γNH 87			
362.5	363.5	βrg 14	τrg 23	νCO 12	βCO 18	βNC 11
349.7	328.1	βrg 19	βCO 18	βCC 19		
328.5	317.5	τrg 88				
313.3	309.1	τrg 38	τNC 46			
313.3	298.2	γOH 72				
278.8	272.0	βrg 14	βCO 26	τCO 12	βCC 14	βNC 11
246.7	253.2	βrg 12	νCO 23	βCO 22	νCC 10	
246.7	248.2	τrg 31	βCO 12	τCO 38		
246.7	243.5	τrg 58	βCO 10			
190.4	196.6	βrg 23	βCO 24	βNC 28		
171.0	165.7	τrg 13	γCH 14	τCO 24	τCC 13	τNC 20
170.7	158.9	γCH 10	τCO 23	τCC 16	τNC 33	
159.7	154.3	τrg 17	γCH 15	τCO 14	τNC 30	
146.7	145.0	τrg 14	γCH 36	τCO 17	τNC 20	
134.2	137.5	τrg 18	τCO 18	τCC 21	τNC 29	
116.7	119.6	βCO 16	τCO 24	βCC 17		
110.7	113.4	νCO 11	βCO 12	τCO 25	νCC 12	
107.3	106.8	τrg 41	τNC 46			
101.6	103.5	βrg 11	βCO 15	τCO 24	τCC 10	βNC 11
94.4	90.9	τCO 14	τNC 59			
83.6	82.4	τCO 72	τNC 11			
55.8	65.0	τrg 31	τCO 11	τCC 34	τNC 15	

(*continued on next page*)

Table 7 (*continued*)

Frequency (cm^{-1})		Potential energy distribution[b] (%)				
Measured[a]	Calculated					
48.1	56.5	βrg 12	βCO 13	τCO 36	βCC 10	τNC 11
45.3	44.9	βCO 12	τCO 32	βCC 10	βNC 12	τNC 20
27.7	33.2	τrg 18	τCO 31	τCC 26	τNC 22	
16.3	18.8	τCO 13	τCC 37	τNC 45		
12.1	14.9	βCO 11	βCC 41	βNC 33		
10.5	7.8	τCO 31	τCC 34	τNC 23		

[a] Measured frequencies for the solid carvedilol.
[b] Distributions not less than 10%; *ν*: stretching; *β*: in-plane deformation; *γ*: out-of-plane deformation: torsion; rg: benzene ring.
[c] carbazole A: CH's for H37 and H42; carbazole B: CH's for H40, H46 and H38; chain A: CH's for H33 and H34; chain B: CH's for H43, H47 and H48; for atom numbering see Fig. 1.

Conclusions

The study of the vibrational spectra of a relatively large molecule with 56 atoms arises several problems especially when the solution spectra are also measured.

One significant problem in the evaluation of solution spectra is the solute–solvent interaction, which becomes apparent upon the subtraction of spectra. In a fortunate case, the interaction is small, which applies to the case described in the present study.

The definition of the internal coordinates (altogether 162) was the next task. The six non-vibrational degrees of freedom were considered with the definition of the coordinates of the single aromatic ring (see Fig. 1).

The appropriate approach to scale the vibrational force constants to the measured vibrational frequencies is to optimize common scale factors for force constants of internal coordinates belonging to similar chemical groups. Such approach applied in the present study yielded useful PEDs.

The comparison of the PED results of the isolated and solute molecules indicated clearly the solvent effects. The solvent effects increased the number of individual (non-coupled) vibrational modes. They were observable in changes of characters of the normal modes, the atomic net charge distributions, vibrational force constants and, as mentioned, in the vibrational frequencies.

Acknowledgement

This work was supported by TUBITAK (the Scientific and Technological Research Council of Turkey) – Science Fellowships and Grant Programmes Department (No. R-R-2227) and HAS (Hungarian Academy of Science) bilateral agreement. It was also supported by the Research Fund of Istanbul University, Project No. BYP/4540.

Appendix A. Supplementary data

Supplementary data associated with this article can be found, in the online version, at http://dx.doi.org/10.1016/j.saa.2012.04.029.

References

[1] <http://en.wikipedia.org/wiki/Carvedilol>.
[2] I. Horiuchi, T. Nozawa, N. Fujii, M. Inoue, M. Honda, T. Shimizu, M. Taguchi, Y. Hashimoto, Biol. Pharm. Bull. 31 (2008) 976–980.
[3] M. Fujimaki, Y. Murakoshi, H. Hakusui, J. Pharm. Sci. 79 (1990) 568–572.
[4] Y. Takekuma, T. Takenaka, K. Yamazaki, K. Ueno, M. Sugawara, Biol. Pharm. Bull. 30 (2007) 2146–2153.
[5] F. Behn, S. Michels, S. Läera, G. Blaschke, J. Chromatogr. B 755 (2001) 111–117.
[6] Xianhong Wen, Fei Tan, Zhijun Jing, Ziuyang Liu, J. Pharm. Biomed. Anal. 34 (2004) 517–523.
[7] D.R.P. Almeida, L.F. Pisterzi, G.A. Chass, L.L. Torday, A. Varro, J. Gy Papp, I.G. Csizmadia, J. Phys. Chem. A 106 (2002) 10423–10436.
[8] D.R.P. Almeida, D.M. Gasparra, T.A. Martinek, F. Fülöp, I.G. Csizmadia, J. Phys. Chem. A 108 (2004) 7719.
[9] L. Jagannathan, R. Meenakshi, S. Gunasekaran, S. Srinivasan, Mol. Simul. 36 (2010) 283–290.
[10] M.P.M. Marques, P-L. Oloveira, A.J.M. Moreno, L.A.E.B. de Carvalho, J. Raman Spectrosc. 33 (2002) 778–783.
[11] W-M. Chen, L.-M. Zeng, K.-B. Yu, J.-H. Xu, Chin. J. Struct. Chem. 17 (05) (1998).
[12] H.S. Yathirajan, S. Bindya, T.V. Sreevidya, B. Narayana, Michael Bolte, Acta Crystallogr. Sect. E 63 (2007) o542–o544.
[13] B. Vajna, G. Patyi, Z. Nagy, A. Bódis, A. Farkas, G. Marosi, J. Raman Spectr., in press, http://dx.doi.org/10.1002/jrs.2943.
[14] M.J. Frisch, G.W. Trucks, H.B. Schlegel, G.E. Scuseria, M.A. Robb, J.R. Cheeseman, J.A. Montgomery Jr., T. Vreven, K.N. Kudin, J.C. Burant, J.M. Millam, S.S. Iyengar, J. Tomasi, V. Barone, B. Mennucci, M. Cossi, G. Scalmani, N. Rega, G.A. Petersson, H. Nakatsuji, M. Hada, M. Ehara, K. Toyota, R. Fukuda, J. Hasegawa, M. Ishida, T. Nakajima, Y. Honda, O. Kitao, H. Nakai, M. Klene, X. Li, J.E. Knox, H.P. Hratchian, J.B. Cross, C. Adamo, J. Jaramillo, R. Gomperts, R.E. Stratmann, O. Yazyev, A.J. Austin, R. Cammi, C. Pomelli, J.W. Ochterski, P.Y. Ayala, K. Morokuma, G.A. Voth, P. Salvador, J.J. Dannenberg, V.G. Zakrzewski, S. Dapprich, A.D. Daniels, M.C. Strain, O. Farkas, D.K. Malick, A.D. Rabuck, K. Raghavachari, J.B. Foresman, J.V. Ortiz, Q. Cui, A.G. Baboul, S. Clifford, J. Cioslowski, B.B. Stefanov, G. Liu, A. Liashenko, P. Piskorz, I. Komaromi, R.L. Martin, D.J. Fox, T. Keith, M.A. Al-Laham, C.Y. Peng, A. Nanayakkara, M. Challacombe, P.M.W. Gill, B. Johnson, W. Chen, M.W. Wong, C. Gonzalez, J.A. Pople, Gaussian 03, Revision C.02, Gaussian, Inc., Wallingford CT, 2004.
[15] A.D. Becke, Chem. Phys. 98 (1993) 5648–5652.
[16] C. Lee, W. Young, R.G. Parr, Phys. Rev. B 37 (1988) 785–789.
[17] R.S. Mulliken, J. Chem. Phys. 23 (1955) 1833–1840.
[18] A.E. Reed, R.B. Weinstock, F.J. Weinhold, J. Chem. Phys. 83 (1985) 735–746.
[19] A.E. Reed, F.J. Weinhold, L.A. Curtiss, Chem. Rev. 88 (1988) 899–926.
[20] M. Cossi, G. Scalmani, N. Rega, V. Barone, J. Chem. Phys. 117 (2002) 43–54.
[21] F. Billes, 2002, unpublished result.
[22] G. Keresztury, S. Holly, G. Besenyei, J. Varga, A. Wang, J.R. Durig, Spectrochim. Acta Part A Mol. Biomol. Spectrosc. 49 (1993) 2007–2026.
[23] G. Yang, Y. Xu, J. Chem. Phys. 130 (2009) 164506-1–164506-9.
[24] G. Yang, Y. Xu, Top. Curr. Chem. 298 (2011) (2011) 189–236.
[25] F. Billes, I. Mohammed-Ziegler, H. Mikosch, Phys. Chem. Chem. Phys. 13 (2011) 7760–7772.
[26] P. Pulay, G. Fogarasi, F. Pang, J. Boggs, J. Am. Chem. Soc. 101 (1979) 2550–2560.
[27] G. Fogarasi, Xuefeng Zhou, P.W. Taylor, P. Pulay, J. Am. Chem. Soc. 114 (1992) 8191–8201.